

## Exploratory Studies in Photomechanics\*

HERBERT BECKER *Allied Research Associates, Concord, Mass.*, and  
ANDREW W. ZACHAR, *Yonkers, New York*

### Synopsis

Exploratory tests were conducted on a specially designed and fabricated photoviscoelastic plastic in order to develop a form for the relationship between fringe order and the mechanical behavior of the plastic. Because of the possible dependence of fringe order upon both stress and strain, the relationship has been termed the photomechanical law. The results which have been obtained so far were inconclusive. In addition, numerous problem areas were discovered which indicate the type of program which may lead to the photomechanical law.

### INTRODUCTION

#### Scope of Project

It is the purpose of this report to describe the results of exploratory studies in photoviscoelasticity. A survey of the historical background reveals rather limited interpretation of the effect of structural behavior on polarized light. As a consequence, preliminary studies have been made in an attempt to broaden this interpretation.

#### Historical Background

Mueller<sup>1</sup> and Mindlin<sup>2</sup> advanced theories of the photoelastic effect in inelastic structures in which it was assumed that the observed birefringence was due either to the elastic component of the structural field or to stress alone. They reported no experiments to test these theories. Stein, Onogi, and Keedy<sup>3</sup> assumed that the total birefringence in a Maxwell body resulted partially from the strain in the spring component and partially from the strain in the dashpot component. No specific stress-dependent effect was assumed. Tests were performed on several plastics to determine experimental data. However, these were not performed in a manner permitting determination of the law of birefringence.

Birefringence in polymeric materials has been investigated experimentally by Kawata<sup>4</sup> and by Andrews and Rudd.<sup>5</sup> However, the emphasis in those studies was not upon development of a relation between birefringence

\* Sponsored by U. S. Navy Department, Office of Naval Research Contract NOnr 285(50).

and structural behavior. This approach was taken recently by Theocaris and Mylonas,<sup>6</sup> who related fringe order to stress level and time.

### Current Program

The approach adopted in this current investigation was guided by a phenomenological approach to a law of birefringence. Data were obtained by photoviscoelastic experiments which were conducted partially to provide a basis for development of a theory and partially to determine the reproducibility of such an experiment. A variation of an epoxy formulation was developed especially for this program to permit observation of photoviscoelastic behavior in the room temperature range.

## THE PHOTOMECHANICAL LAW

### Elastic Material

If a perfectly elastic isotropic material exhibits significant temporary birefringence under stress, then the law relating the two for uniaxial stress is usually formulated in terms of fringe order  $n$ , as

$$n = C_\sigma \sigma = K \Delta \quad (1)$$

where  $C_\sigma$  and  $K$  are material constants. The relative retardation,  $\Delta$ , usually is explained on the basis of a change in refractive index in the direction of the stress,  $\sigma$ .

Since stress is proportional to strain  $\epsilon$ , then it is also legitimate to write

$$n = C_\epsilon \epsilon \quad (2)$$

where naturally

$$C_\epsilon = EC_\sigma$$

Equation (1) is the stress-optic law, while eq. (2) is the strain-optic law for the material. Actually, in the general case of a biaxial field,  $\Delta$  is a difference in retardation charged to the difference in indices of refraction in the principal stress directions and  $\sigma$  is the difference in principal stresses. However, use of eq. (1) has the advantage of simplicity in what is to follow.

### The Photomechanical Law

Goodman and Sutherland,<sup>7</sup> on investigating birefringence in silver chloride crystals, found a linear relation between stress and retardation but not between strain and retardation. They explained this on the basis of a law of the form of eq. (1) operating in the crystal grains both before and after slip, and found that the consequent nonlinear relation between stress and strain was reflected in a nonlinear strain-optic relation.

This is one factor in a controversy which has continued for decades. Investigators have asked whether structural birefringence is related to stress or to strain. In the preceding case it appears to be stress-related.

In certain types of crystals it is known to be strain-related. These are essentially clear-cut cases. The controversy is most difficult to resolve for noncrystalline materials such as those which could be useful in photo-viscoelasticity.

For this reason the term "photomechanical law" is adopted in this report to signify the relation between birefringence and mechanical behavior, and the generic term for the field of study is termed "photomechanics."

### Viscoelasticity

The two extremes of structural behavior in the current field of investigation are (1) elasticity and (2) viscosity. They may be broadly identified as (1) stress proportional to strain and 100% recovery upon unloading, and (2) stress proportional to strain rate and zero recovery upon unloading. The field of viscoelasticity embraces the behavior domain bounded by these limits.

Many viscoelastic structures are linearly viscoelastic, as expressed in the form (for purely time-dependent behavior)

$$P(\sigma) = Q(\epsilon) \quad (3)$$

where

$$P = \sum p_r D^r \quad (4)$$

$$Q = \sum q_s D^s \quad (5)$$

where  $D = d/dt$  and  $p_r, q_s$  are constants. Naturally, these meet the limiting conditions, that is,

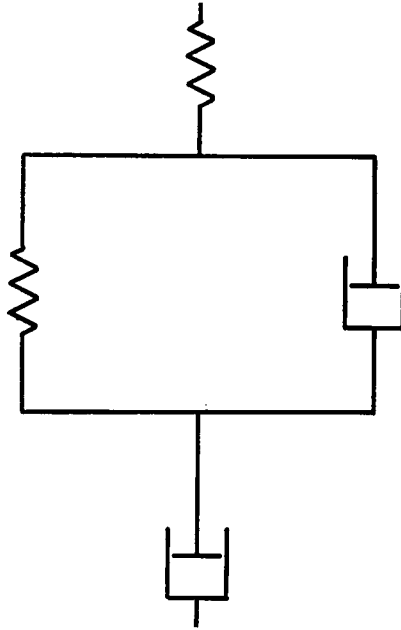
$$\sigma = (q_0/p_0)\epsilon = E\epsilon \quad \text{when } r = s = 0 \quad (6)$$

$$\begin{aligned} \sigma &= (q_1/p_0)(d\epsilon/dt) \quad \text{when } r = 0, & (7) \\ &= cd\epsilon/dt \quad \quad \quad \quad \quad \quad \quad s = 1 \end{aligned}$$

The relationship between stress and strain exemplified by eq. (3) is generally found to be satisfied in a relatively simple form for elementary structural models or for complex models as long as the time range is confined to one or two decades of behavior. A simple model would be the Maxwell or Voigt body, or a combination of the two. Mindlin utilized the latter situation (Fig. 1) in developing his theory of photoviscoelasticity. For larger time ranges, more complex models are generally required, and corresponding increase in the complexity of eq. (3) occurs. This is discussed to some extent by Ferry<sup>8</sup> and by Bland,<sup>9</sup> for example.

### Photoviscoelasticity

One limiting phenomenon of this field of photomechanics is photoelasticity which requires no documentation beyond that discussed above. The other is photoviscosity which involves birefringence produced by shear stresses in a viscous fluid. Weller, Middlehurst, and Steiner,<sup>10</sup> for example,

Fig. 1. Model used by Mindlin.<sup>2</sup>

described an experiment to demonstrate this phenomenon in which fringe patterns are photographed to reveal the flow patterns in the fluid. Consequently birefringence could be caused by either the elastic or viscous component in a viscoelastic structure such as shown in Figure 1.

It is well known that fringe changes will occur in almost any photoelastic model under high loading if that load is permitted to remain on the model for a long time. Consequently, fringe order in a viscoelastic structure could be changed both to stress and to strain. Furthermore, the possible presence in the material of a photoviscous effect could induce fringes as a result of strain rate. Therefore it is conceivable that the photomechanical law for a viscoelastic structure would be

$$n = C_{\sigma}\sigma + C_{\epsilon}\epsilon + C_{D_{\epsilon}}D\epsilon \quad (8)$$

If the material is linearly viscoelastic then it might also be linearly photoviscoelastic. That is, in general

$$P(n) = V(\epsilon) \quad (9)$$

$$P = \Sigma p_r D^r \quad (10)$$

$$V = \Sigma v_a D^a \quad (11)$$

Equation (8) sheds an interesting light upon birefringence in an elastic material. In that case strain rate effects would vanish and

$$n = C_{\sigma}\sigma + C_{\epsilon}\epsilon \quad (12)$$

or possibly

$$n = A\sigma \quad (13)$$

if there is an attempt to construct a stress-optic law. Actually, then,

$$\begin{aligned} A\sigma &= C_\sigma\sigma + C_\epsilon\epsilon \\ &= C_\sigma\sigma + C_\epsilon\sigma/E \end{aligned} \quad (14)$$

or

$$A = C_\sigma + C_\epsilon/E \quad (15)$$

In other words, this leaves room for the possibility that part of the observed birefringence in an elastic photomechanical material may be due to stress and part to strain.

### EXPERIMENTAL PROCEDURE

The approach adopted in this exploratory study of photomechanics included experimental studies of stress, strain, time, temperature, and fringe order for a representative viscoelastic epoxy, and an evaluation of a similar investigation conducted by Theocaris and Mylonas.<sup>6</sup> In addition, an attempt was made to relate fringe order to the mechanical behavior

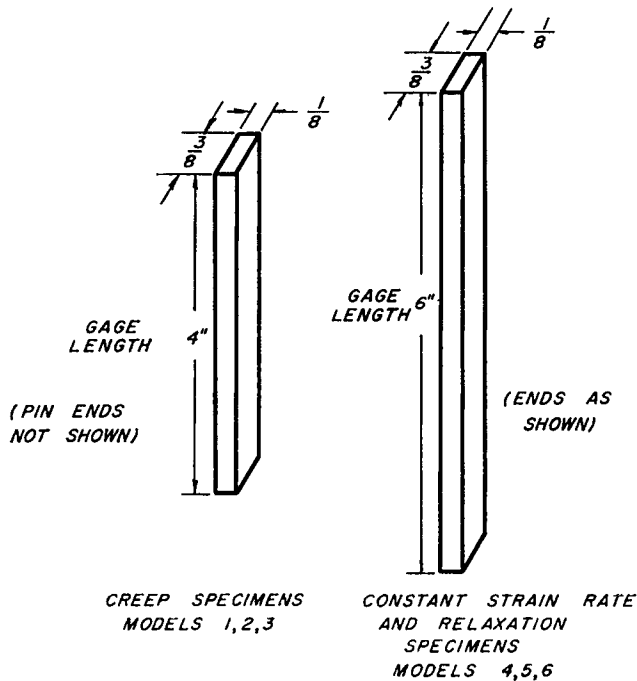


Fig. 2. Specimen dimensions.

according to eqs. (8) and (12). For the present the investigation was confined to uniaxial stresses.

Hysol 4290 is viscoelastic at 275°F. However, this is an inconvenient temperature for performance of the experiments in this program. Con-

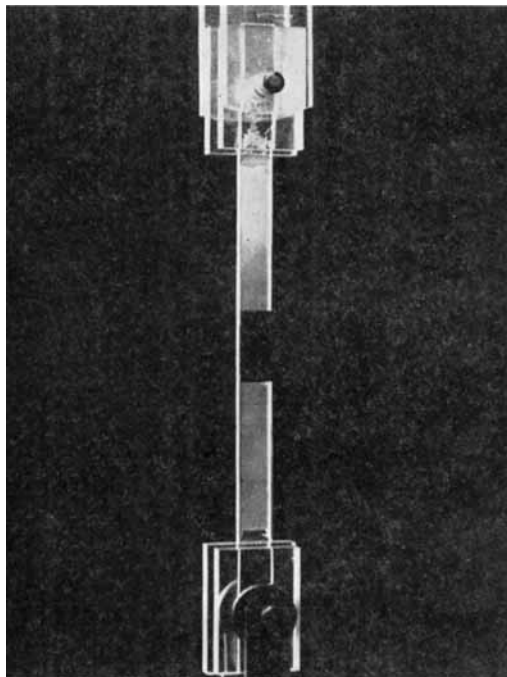


Fig. 3. Detail of pin-ended creep specimen.

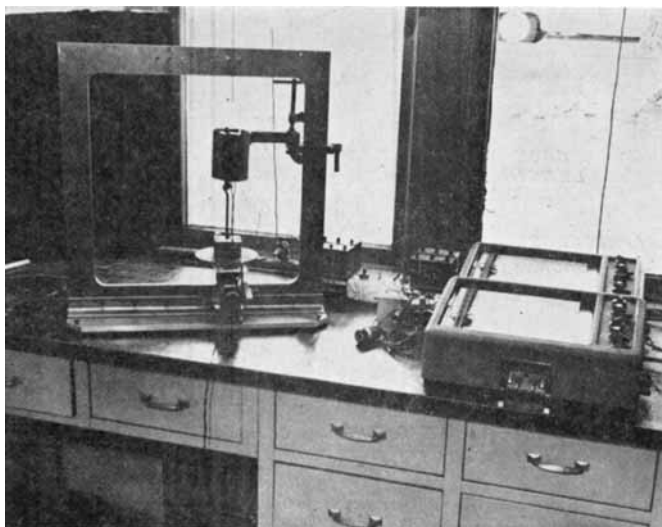


Fig. 4. Assembly of creep apparatus.

sequently, after a series of exploratory tests to find a suitable material, Hysol XCP-C467 was selected for study. This is essentially Hysol 4290 to which 30% (by weight of monomer) urethane rubber has been added to provide viscoelastic behavior in the temperature range 60–110°F. Six tensile specimens of the dimensions shown in Figure 2 were machined from a 12-in. square plate of this material. These specimens were selected from various locations in the plate to check possible variations in material property.

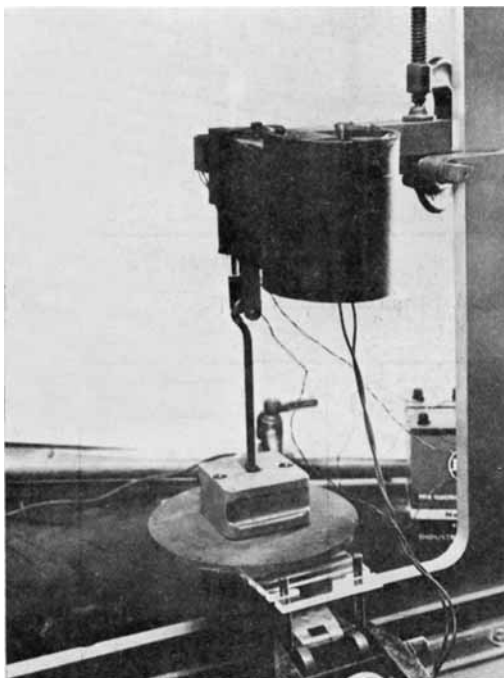


Fig. 5. Detail of loading arrangement in creep apparatus.

Three types of tests were performed: constant dead load tensile stress, constant tensile strain rate, and constant tensile strain. The dead load tests were performed in the apparatus shown in Figures 3–5, while the other tests were performed in an Instron tensile tester.

## EXPERIMENTAL DATA

### Constant Stress (Creep)

Creep tests were performed on three identical specimens  $\frac{1}{8}$  in. thick,  $\frac{3}{8}$  in. wide, and approximately 4 in. long. The experiments were conducted under dead load, the equipment shown in Figures 4 and 5 being used. The specimens were cut from different locations in a single  $12 \times 12 \times \frac{1}{2}$  in. sheet of 30% plasticized epoxy, type XCP-C467.

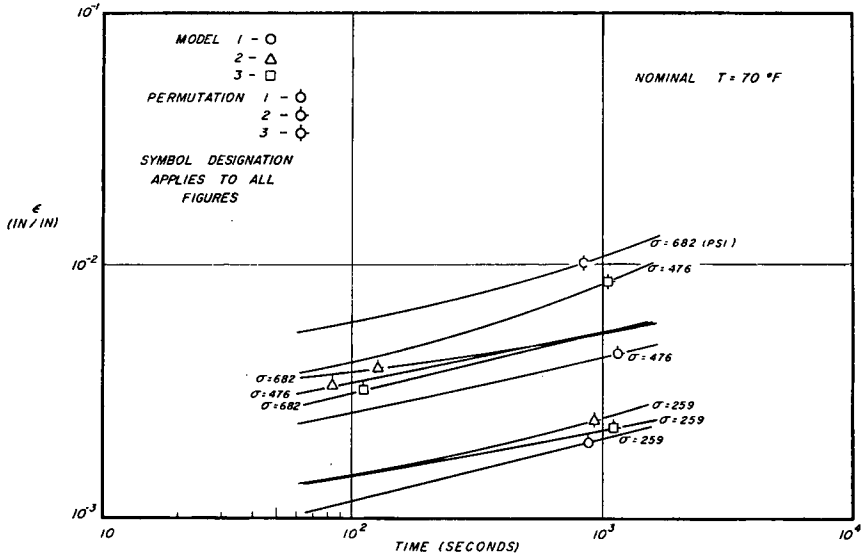


Fig. 6. Strain data under creep. Nominal  $T = 70^{\circ}\text{F}$ .

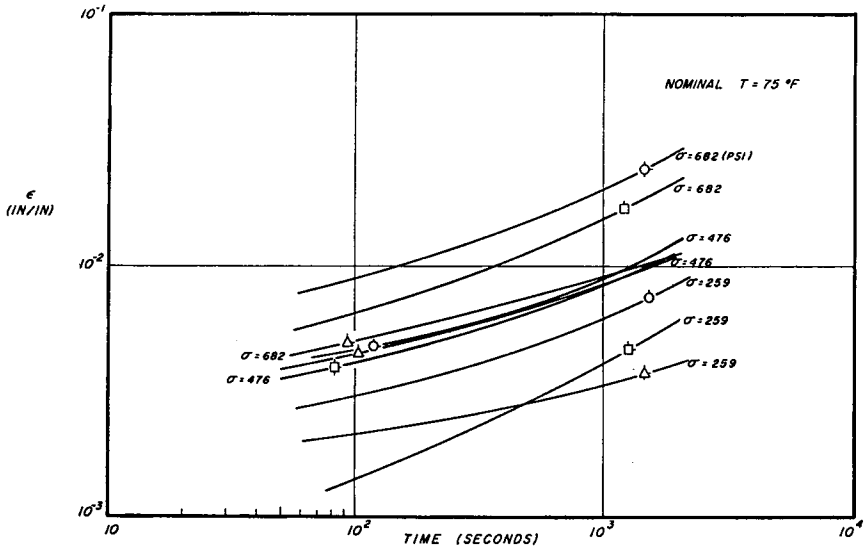


Fig. 7. Strain data under creep. Nominal  $T = 75^{\circ}\text{F}$ .

Tests were run at approximately 70, 75, and 80°F. Strain and fringe order were recorded as functions of time. The models (annealed and measured before each test) were loaded in cyclic permutation at each temperature level. The model dimension measurements indicated no obvious residual effects due to the previous loading condition and the annealing process. Initial strains were always less than 0.0001. Further-



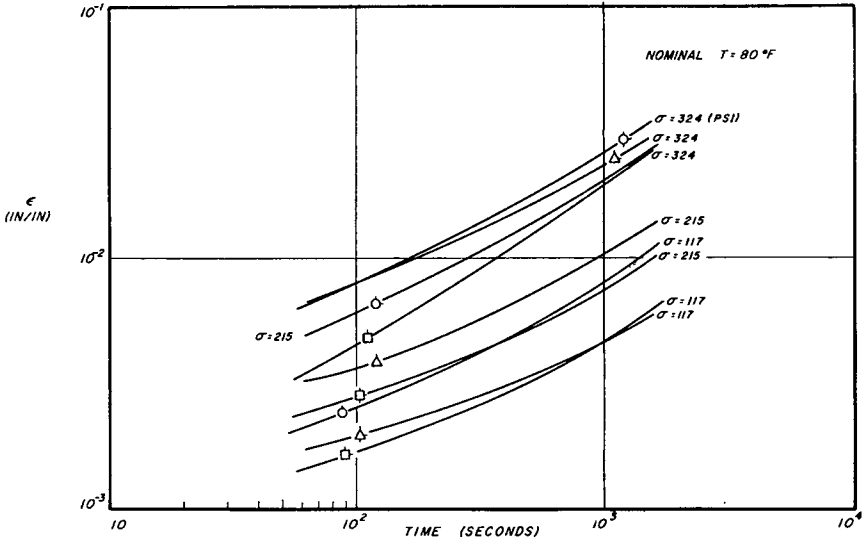


Fig. 8. Strain data under creep. Nominal  $T = 80^\circ\text{F}$ .

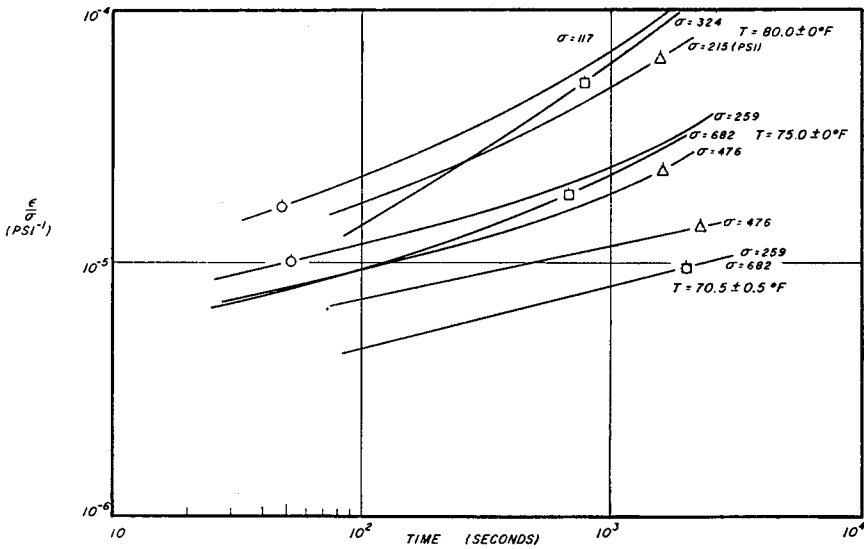


Fig. 9. Stress-normalized creep strain data. First permutation.

more, in every case initial fringe orders were within 0.1 fringes of zero fringe order.

Table I contains a summary of the current test conditions. Results are shown in Figures 6-19.

The experimental data exhibited wide scatter, as may be seen in the stress-normalized curves of Figures 9-11 and 15-17. Some of the possible causes of scatter are discussed in a subsequent section. Creep data found

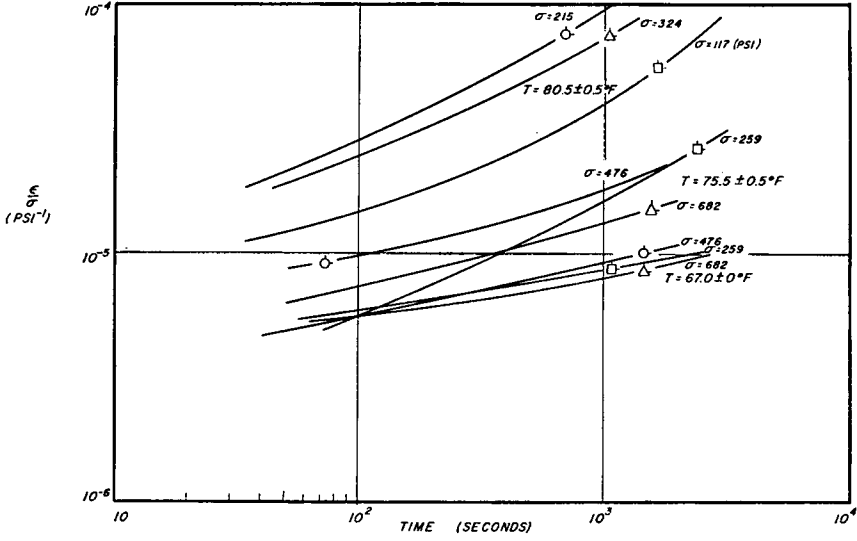


Fig. 10. Stress-normalized creep strain data. Second permutation.

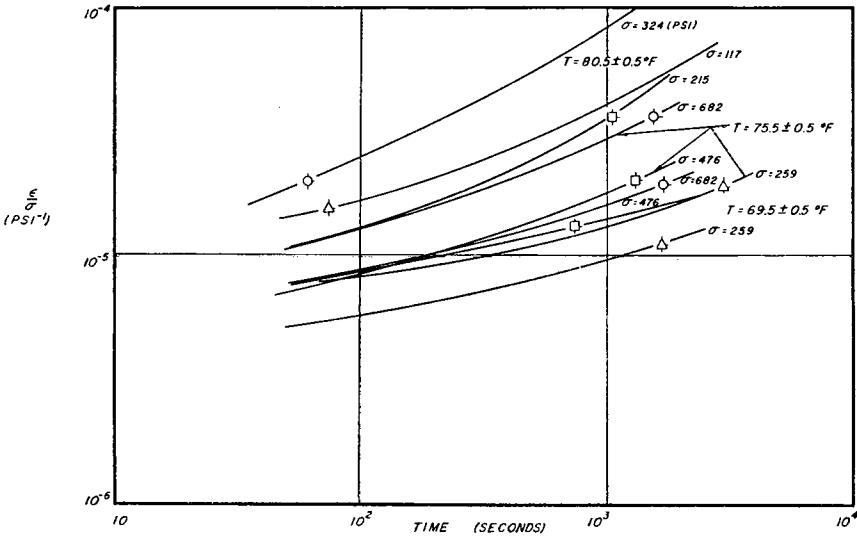
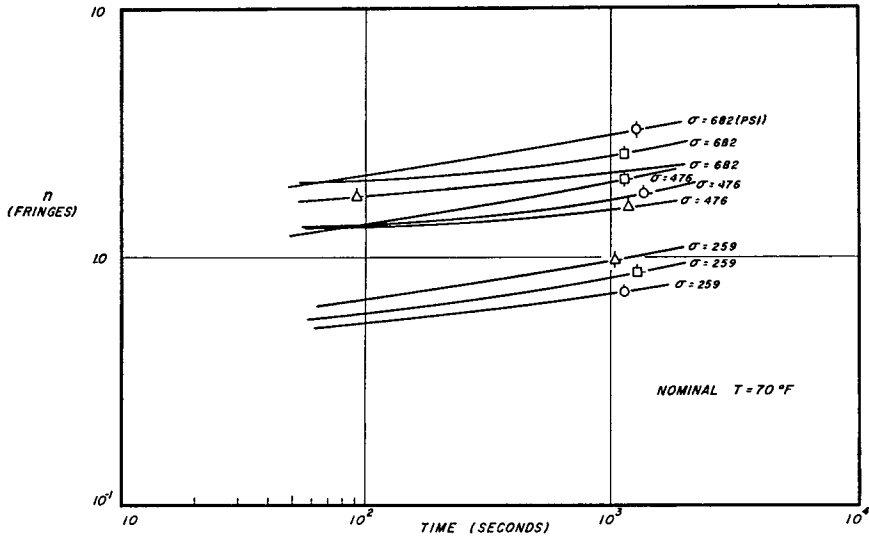
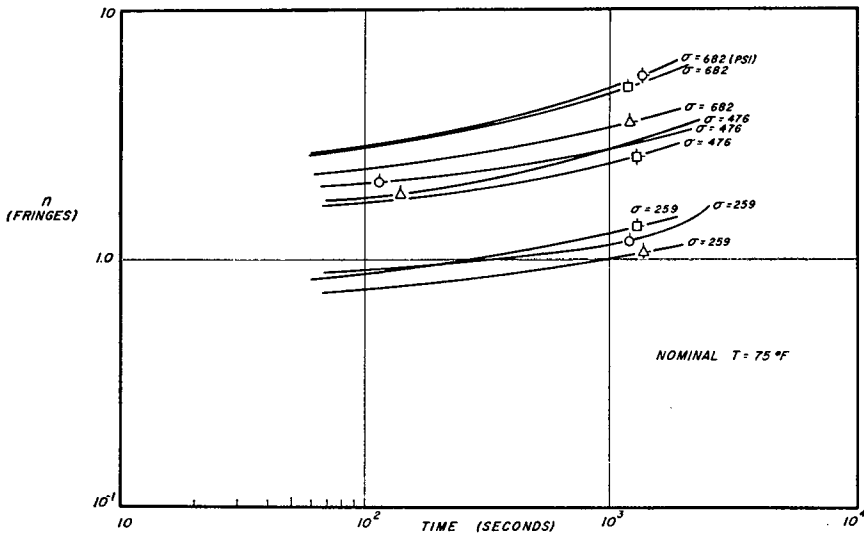


Fig. 11. Stress-normalized creep strain data. Third permutation.

by Theocaris and Mylonas<sup>6</sup> are presented in Figures 18 and 19. The relatively small strain range of their tests is noteworthy.

### Constant Strain Rate

The constant strain rate tests (and the constant strain tests to be described below) on the models 4, 5, and 6 shown in Figure 20 (dimensions appear in Fig. 2) were performed in an Instron tensile tester. The experi-

Fig. 12. Fringe-order data under creep. Nominal  $T = 70^\circ\text{F}$ .Fig. 13. Fringe order data under creep. Nominal  $T = 75^\circ\text{F}$ .

mental arrangement is shown in Figures 21 and 22. A set of tests was performed at  $78^\circ\text{F}$ ., principally to explore the problems involved in obtaining reliable data from this type of test.

One of the principal problems was accurate control of the strain in the model. It was found that the pin end design on the creep specimens made it impossible to obtain a predictable relation between model strain and the crosshead motion of the machine. It was necessary to redesign the model

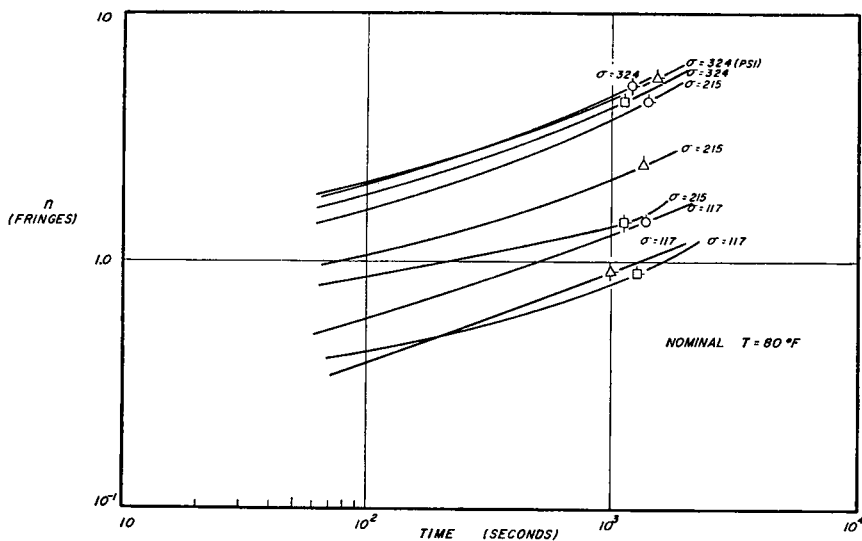


Fig. 14. Fringe order data under creep. Nominal  $T = 80^\circ\text{F}$ .

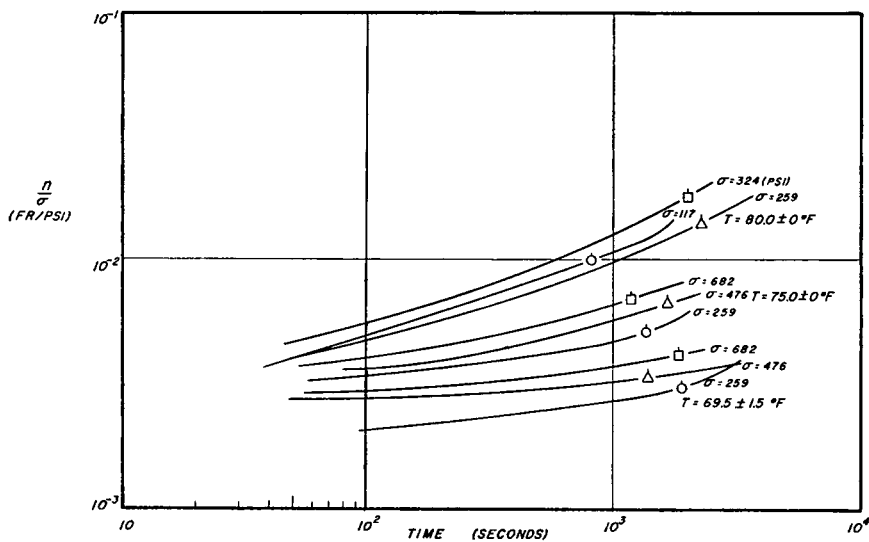


Fig. 15. Stress-normalized creep fringe order data. First permutation.

and load transfer equipment in order to obtain correlation of these two factors. Since the prime purpose of this test was to examine the behavior of the photoviscoelastic material under constant strain rate, this correlation was a basic requirement.

The desired result was obtained by utilizing specimens with square ends. These were attached by cementing to rugged steel load transfer cylinders (see Fig. 20). These cylinders were pinned into the Instron crosshead and

TABLE I  
Photoviscoelastic Creep Test Conditions

Model no.	T, °F.	σ, psi	T, °F.	σ, psi	T, °F.	σ, psi
1	80.0	117	75.0	259	69.5	259
2	80.0	215	75.0	476	69.5	476
3	80.0	324	75.0	682	69.5	682
1	80.5	215	75.5	476	67.0	476
2	80.5	324	75.5	682	67.0	682
3	80.5	117	75.5	259	67.0	259
1	80.5	324	75.5	682	69.5	682
2	80.5	117	75.5	259	69.5	259
3	80.5	215	75.5	476	69.5	476

TABLE II  
Photoviscoelastic Constant Strain Rate Test Conditions

Model no.	T, °F.	Dε × 10 <sup>3</sup> , sec. <sup>-1</sup>
4	78	0.278
5	78	0.557
6	79	1.39

into the loading cell. Upon completion of this modification, excellent correlation was obtained between crosshead motion and specimen strain. (Equipment shown in Figs. 21 and 22.)

The test conditions are summarized in Table II.

The experimental results appear in Figures 23 and 24.

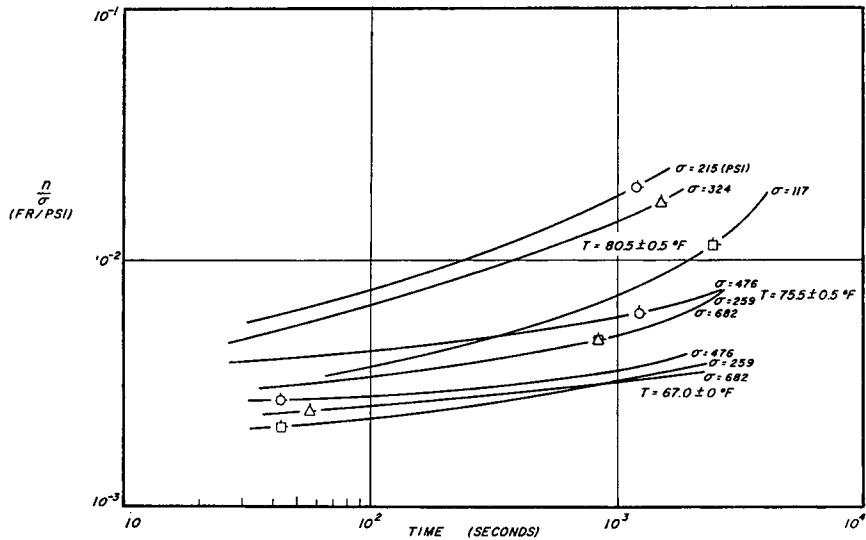


Fig. 16. Stress-normalized creep fringe order data. Second permutation.

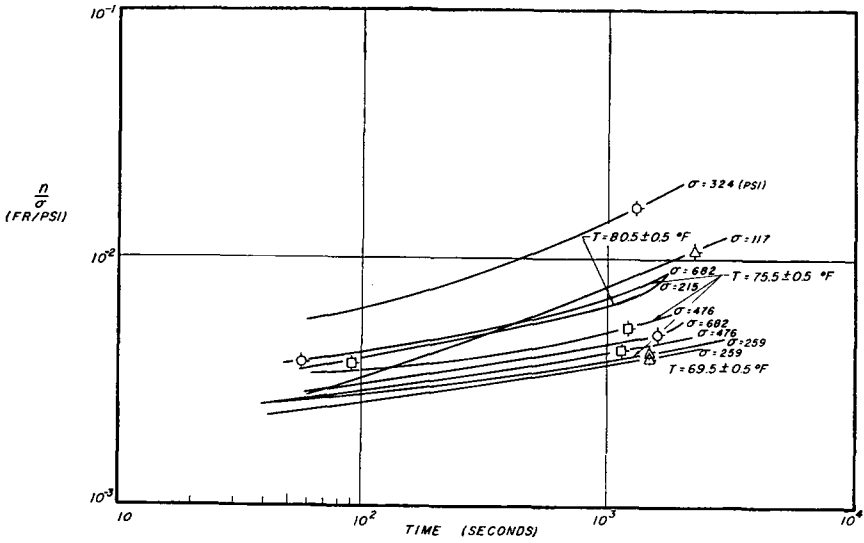


Fig. 17. Stress-normalized creep fringe order data. Third permutation.

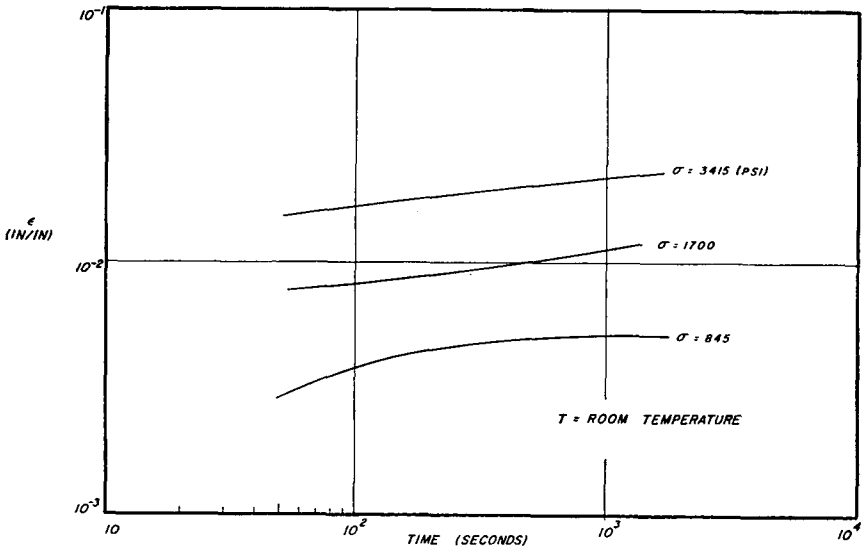


Fig. 18. Strain data under creep (data of Theocaris and Mylonas<sup>6</sup>).

### Constant Strain (Relaxation)

The constant strain tests also required close correlation between model strain and crosshead motion. In preliminary tests on the creep specimens before they were modified, specimen strain could not be maintained constant after cessation of crosshead motion. After modification as discussed previously, specimen strain was accurately maintainable at the value which existed when the crosshead was halted.

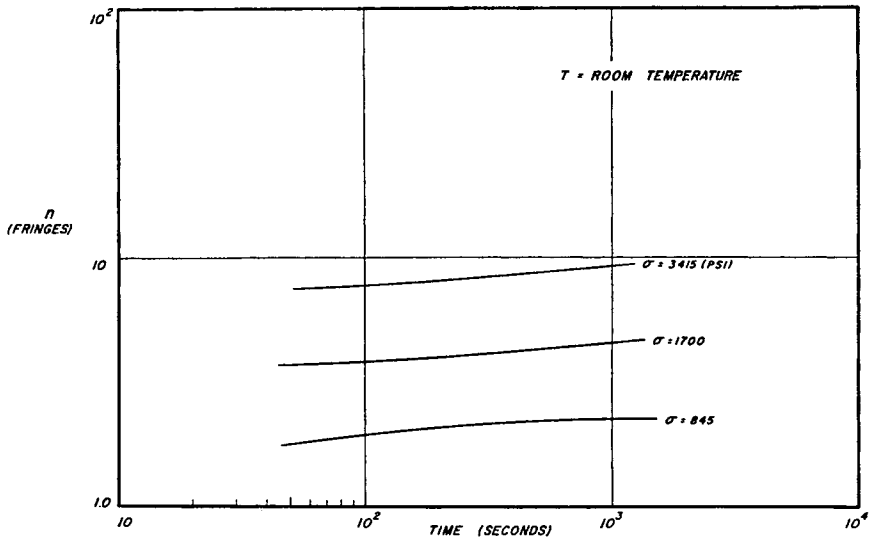


Fig. 19. Fringe order data under creep (data of Theocaris and Mylonas<sup>6</sup>).

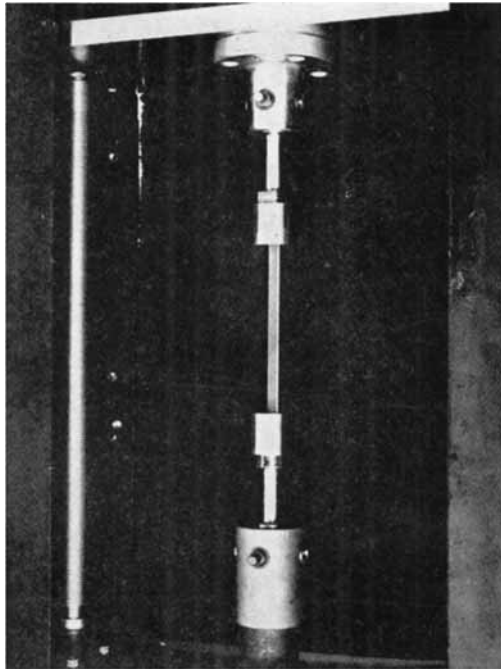


Fig. 20. Specimen for constant strain rate and relaxation tests shown end-cemented to rugged load transfer members.



Fig. 21. Assembly of apparatus for controlled strain and strain rate tests.

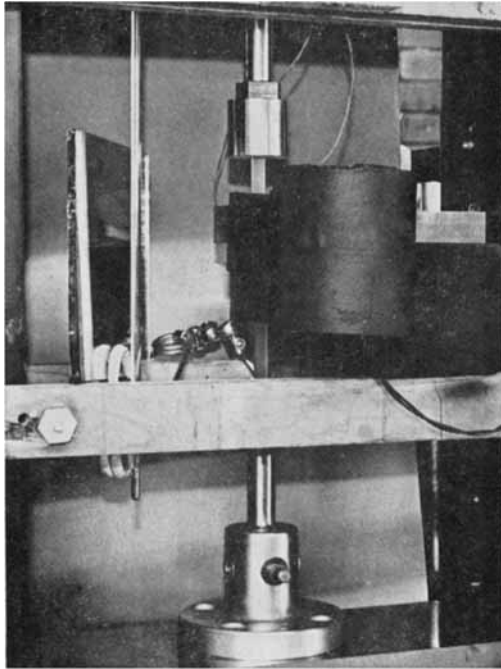


Fig. 22. Detail of loading arrangement for controlled strain and strain rate tests.



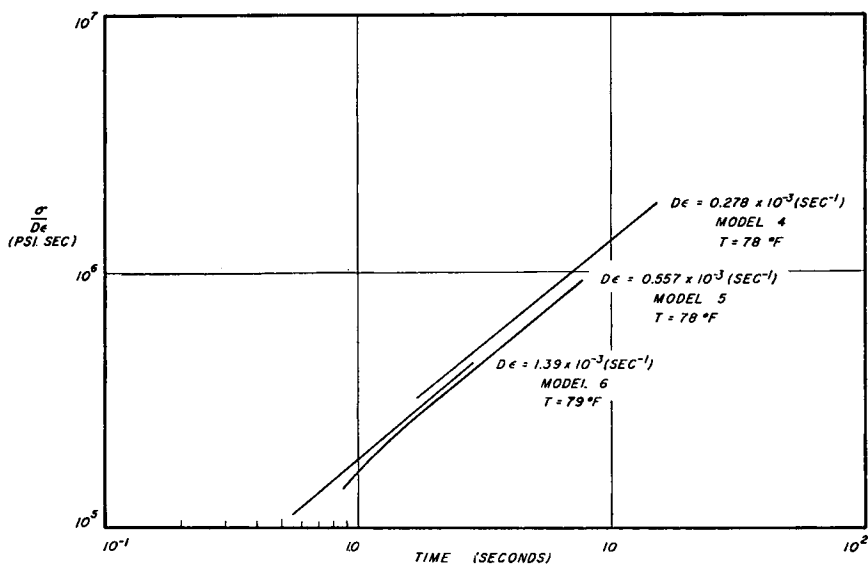


Fig. 23. Strain rate-normalized stress data during constant strain rate tests (see Fig. 25 for unnormalized data).

The test conditions are summarized in Table III.

TABLE III  
Photoviscoelastic Relaxation Test Conditions<sup>a</sup>

Model no.	$T$ , °F.	$\epsilon_0$	$\sigma_0$
4	78	0.00420	500
5	78	0.00433	513
6	79	0.00391	529

<sup>a</sup>  $\epsilon_0$ ,  $\sigma_0$  refer to condition at start of test.

The test data appear in Figures 25 and 26. Relaxation data of Theocaris and Mylonas<sup>6</sup> are presented in Figures 27 and 28.

### DETERMINATION OF PHOTOMECHANICAL LAW

In spite of the scatter in the data, an attempt was made to determine the coefficients for several simple photomechanical laws. The results of these investigations are presented below.

#### Elastic Type Law

The first attempt to evolve a photomechanical law entailed the use of eqs. (1) and (2), which specify dependence of fringe order directly upon stress and upon strain, respectively. The data appear in Table IV.

TABLE IV  
Fringe Order as a Function of Stress or of Strain  
( $n = C_{\sigma}\sigma$  or  $n = C_{\epsilon}\epsilon$ ) Creep Data

Test no.	Temp., °F.	Stress, psi	Model no.	$C_{\sigma}$ , fringes/psi	$C_{\epsilon}$ , fringes
1	80.0	117	1	0.0110	161
2	80.0	215	2	0.0099	202
3	80.0	324	3	0.0129	211
4	75.0	259	1	0.0047	197
5	75.0	476	2	0.0058	309
6	75.0	682	3	0.0067	299
7	69.5	259	1	0.0028	339
8	69.5	476	2	0.0033	279
9	69.5	682	3	0.0038	462
10	80.5	117	3	0.0071	178
11	80.5	215	1	0.0175	182
12	80.5	324	2	0.0140	194
13	75.5	259	3	0.0049	306
14	75.5	476	1	0.0058	324
15	75.5	682	2	0.0049	366
16	67.0	259	3	0.0033	378
17	67.0	476	1	0.0038	388
18	67.0	682	2	0.0032	400
19	80.5	117	2	0.0078	195
20	80.5	215	3	0.0065	183
21	80.5	324	1	0.0143	173
22	75.5	259	2	0.0039	298
23	75.5	476	3	0.0051	287
24	75.5	682	1	0.0070	237
25	69.5	259	2	0.0038	387
26	69.5	476	3	0.0042	300
27	69.5	682	1	0.0045	281

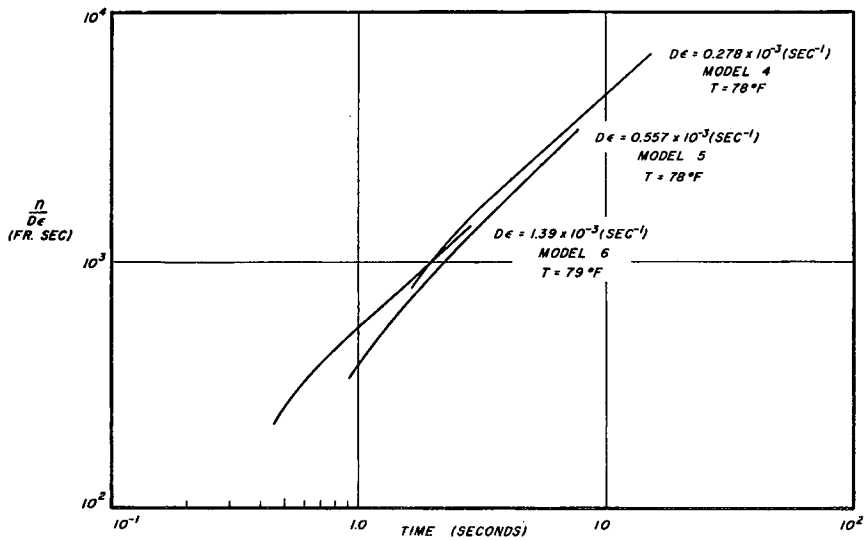


Fig. 24. Strain rate-normalized fringe-order data during constant strain rate tests (see Fig. 26 for unnormalized data).

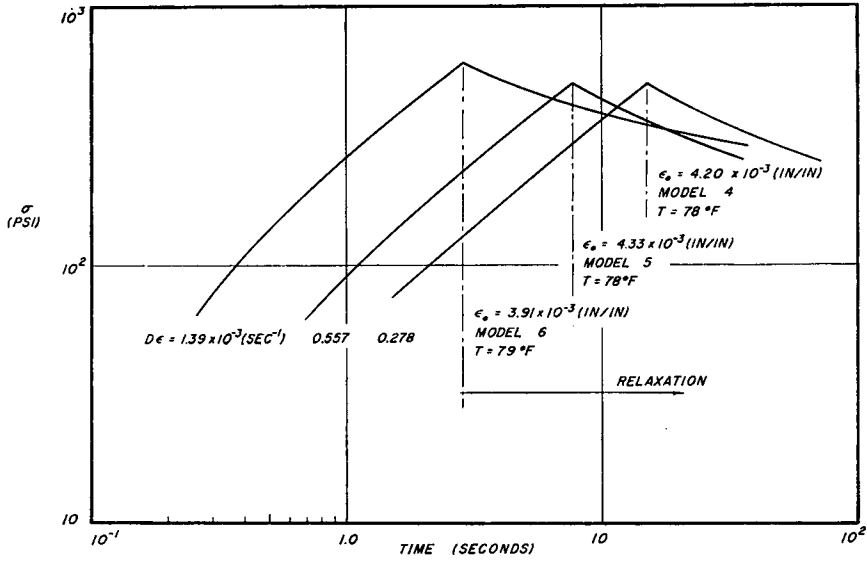


Fig. 25. Stress data under relaxation.

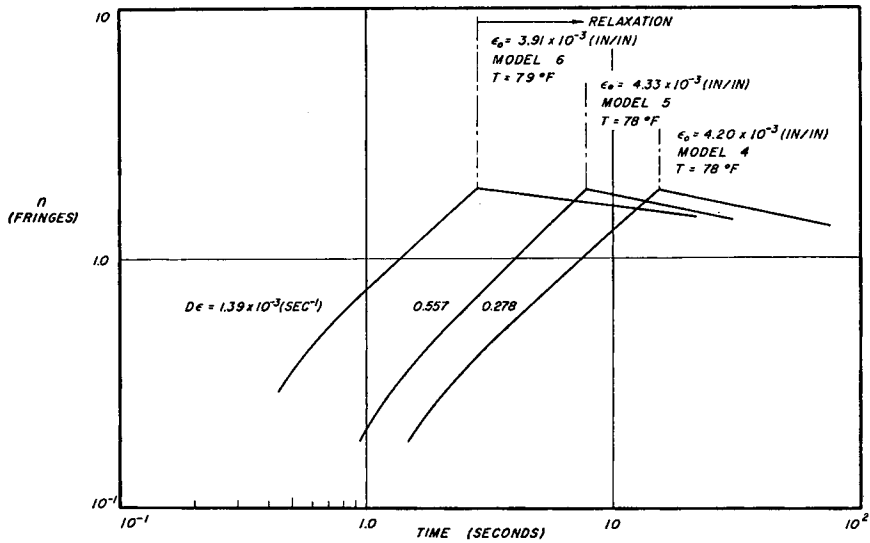


Fig. 26. Fringe order data under relaxation.

As may be seen, little success was achieved in obtaining constant values for  $C_\sigma$  and  $C_\epsilon$ , as was to be expected.

**Stress- and Strain-Dependent Law**

A slightly more involved relation was examined utilizing eq. (12) in which fringe order is linearly related to both stress and to strain. As the results in Table V show, a slight improvement was achieved.

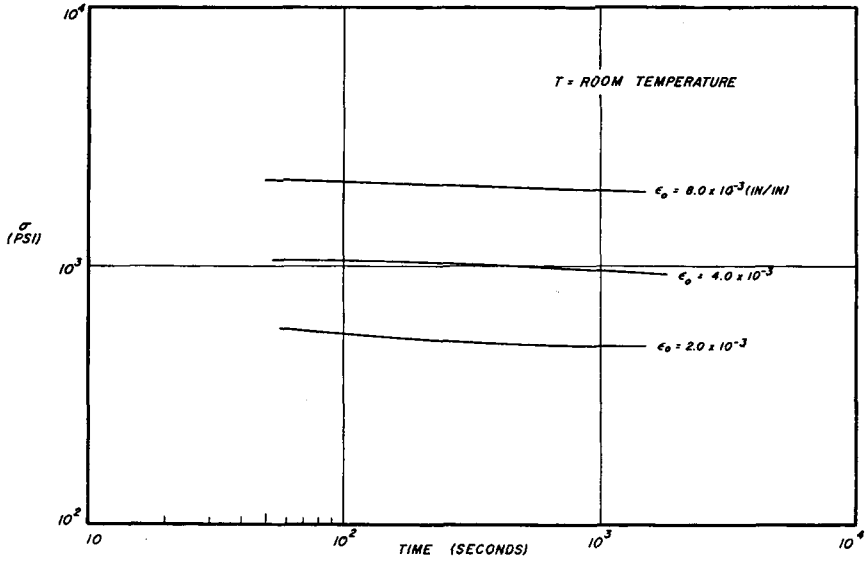


Fig. 27. Stress data under relaxation (data of Theocaris and Mylonas<sup>6</sup>).

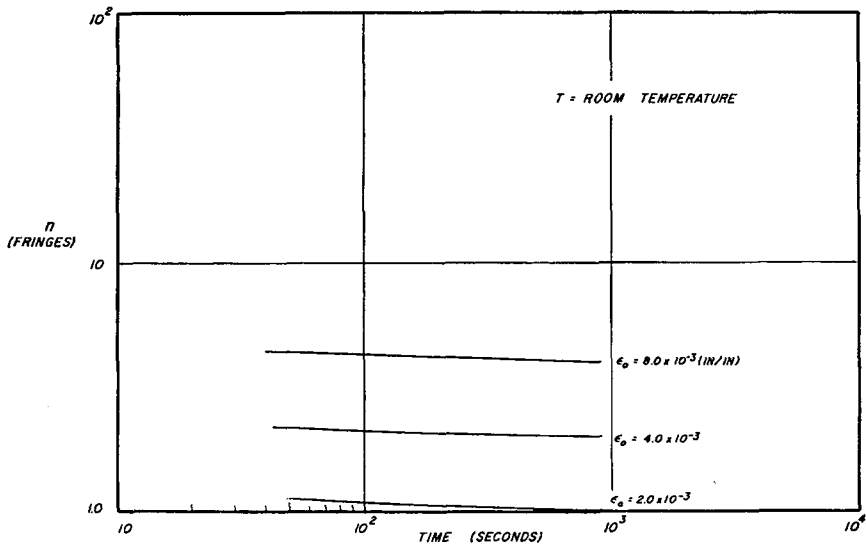


Fig. 28. Fringe order data under relaxation (data of Theocaris and Mylonas<sup>6</sup>).

For the case of relaxation on the specimens 4, 5, and 6 relatively good agreement was obtained. In this set of tests the three stress coefficients agree within comparatively small scatter, as do the strain coefficients. Actually, all strain derivatives vanish for this test. However, time derivatives of stress and fringe order could be significant. It is still too early to tell whether this result has meaning or is merely fortuitous.

TABLE V  
Fringe Order as a Function of Both Stress and Strain  
( $n = C \sigma + C \epsilon$ )

Test no.	Temp., °F.	Stress, psi	Model no.	$D\epsilon \times 10^3$ , sec. <sup>-1</sup>	$\epsilon \times 10^3$ , in./in.	$C_\sigma \times 10^3$ , fringes/psi	$C_\epsilon$ , fringes
Creep Data							
1	80.0	117	1			2.149	129.6
2	80.0	215	2			2.243	156.3
3	80.0	324	3			3.555	153.2
4	75.0	259	1			2.231	104.1
5	75.0	476	2			1.350	250
6	75.0	682	3			2.185	201.6
7	69.5	259	1			1.246	185.7
8	69.5	476	2			2.048	104.4
9	69.5	682	3			2.014	214.3
10	80.5	117	3			1.767	133.3
11	80.5	215	1			3.222	148.7
12	80.5	324	2			2.608	158.2
13	75.5	259	3			2.614	142.9
14	75.5	476	1			2.485	185.2
15	75.5	682	2			1.605	245.9
16	67.0	259	3			0.332	339.3
17	67.0	476	1			1.655	208.1
18	67.0	682	2			1.200	250.0
19	80.5	117	2			0.008	194.8
20	80.5	215	3			2.538	111.6
21	80.5	324	1			2.863	138.6
22	75.5	259	2			1.226	204.1
23	75.5	476	3			2.198	163.0
24	75.5	682	1			2.007	168.7
25	69.5	259	2			0.961	287.5
26	69.5	476	3			0.766	245.3
27	69.5	682	1			2.831	191.8
Constant Strain Rate Data							
	78		4	0.278		1.94	208
	78		5	0.557		-0.62	539
	78		6	1.39		1.304	284
Relaxation Data							
	78		4		4.20	2.67	135.3
	78		5		4.33	2.51	139.0
	78		6		3.91	2.19	136.9
*	Room				8	2.38	-82.5
*	tem-				4	2.22	-42.5
*	pera-				2	0.98	279
	ture						

\* Data of Theocaris and Mylonas<sup>6</sup>

### Inclusion of Strain Rate

The final synthesis of the data utilized eq. (8), which includes the possibility of strain-rate sensitivity. As Table VI shows, there is little point in attempting to interpret the results at this stage.

## CAUSES OF SCATTER IN DATA

The major sources of error in measuring the response of a viscoelastic material would be expected to arise from the sensitivity of the material

TABLE VI  
Fringe Order as a Function of Stress, Strain, and Strain Rate  
( $n = C_\sigma + C_\epsilon \epsilon + C_{D\epsilon} D\epsilon$ )

Test no.	Temp., °F.	Stress psi	Model no.	$(D\epsilon)_0 \times 10^3, \text{sec.}^{-1}$	$C_\sigma \times 10^3, \text{fringes/psi}$	$C_\epsilon$ fringes	$C_{D\epsilon} \times 10^3$ fringe-sec.
Creep Data							
1	80.0	117	1		5.41	102	-32.3
2	80.0	215	2		3.30	143	-15.0
3	80.0	324	3		4.49	144	-10.2
4	75.0	259	1		-0.426	192	54.0
5	75.0	476	2		1.03	248	14.4
6	75.0	682	3		2.13	205	-0.69
7	69.5	259	1		1.19	194	1.51
8	69.5	476	2		3.25	8.58	-34.1
9	69.5	682	3		1.24	304	35.9
10	80.5	117	3		2.05	129	-5.30
11	80.5	215	1		4.64	140	-9.17
12	80.5	324	2		4.07	144	-11.2
13	75.5	259	3		2.82	135	-7.78
14	75.5	476	1		2.68	177	-6.92
15	75.5	682	2		1.07	283	12.0
16	67.0	259	3		-0.371	415	28.7
17	67.0	476	1		0.656	308	43.2
18	67.0	682	2		1.36	233	-12.0
19	80.5	117	2		2.36	154	-36.6
20	80.5	215	3		8.96	51.3	-201
21	80.5	324	1		3.43	135	-4.84
22	75.5	259	2		1.68	170	-13.4
23	75.5	476	3		1.93	175	5.27
24	75.5	682	1		2.27	161	-4.03
25	69.5	259	2		0.922	301	-3.56
26	69.5	476	3		0.953	232	-6.01
27	69.5	682	1		2.18	155	-22.4
a	Room tem-	3415			0.512	342	282
a	perature	1700			1.1	241	9.5
a		845			1.68	165	-244
Constant Strain Rate							
78			4	0.278	3.9	-17.5	-323
78			5	0.557	-0.875	570	17
78			6	1.39	-1.43	657	159

\* Data of Theocaris and Mylonas.<sup>6</sup>

to its environment and from the manner of loading. The secondary sources such as dimensions and loads, or fringe orders and strains, lead to errors in the order of a few per cent at most.

### Temperature Effects

In the region of the transition from a stiff glassy structure to a flexible elastic structure, photoelastic materials are known to be sensitive to changes in temperatures. During the tests which were performed in this exploratory program the temperature changes in the atmosphere surrounding each specimen varied from  $\pm 0.5^{\circ}\text{F.}$  to  $\pm 1^{\circ}\text{F.}$  about each mean test temperature.

A precise determination of this effect would require precise temperature control, which was not attempted in these exploratory tests. Some measure of the temperature sensitivity may be obtained from observation of the curves of strain as a function of time. These are summarized in Figures 6-8 which reveal a total nominal temperature range of  $10^{\circ}\text{F.}$  within which all tests were run.

### Humidity Effects

The stress-optic behavior of initially dry photoelastic material after introduction into a moist atmosphere is well known. The behavior is known as "time effect." It has been explained by gradual transport of moisture from the model-atmosphere interface into the interior of the model, leading to surface expansion restrained by the interior with consequent stresses which change with time.

If one were to speculate as to the possible effect upon mechanical properties of this moisture transport, it could be conjectured that internal structural changes on a molecular level might be expected. In any event, there may be reason to suspect (on this basis) that humidity could affect appreciably the creep characteristics of photoelastic plastics in the viscoelastic temperature range. Quantitative studies on this effect are notably scarce. Evidently, data on this factor must await further investigation.

### Manner of Loading

During the creep tests a dead weight load was supported on a platform which was lowered away from the model by hand control to initiate the test. No measurement was made of the load buildup on the model. In every case the entire load was transferred to the model within roughly 0.5 sec. Discussions with independent investigators have indicated that the effect of the details of the initial loading should be minimized within two time decades after load application. This behavior was not observed in the current tests, as may be seen in Figures 8-11 and 15-17.

### Model Structure

Photoelastic plastics are noted for variations in material properties. Elastic modulus and material fringe value have been known to vary by more than 10% above or below average values published in the literature. Variation occurs from batch to batch, and may even be found to be significant throughout a 12 inch square plate.

It is not surprising therefore, that material property data exhibit large variations in the viscoelastic range of materials which have had extensive applications in photoelasticity. The explanation of this behavior may be found in the material structure variations associated with the degree of polymerization and the purity of the chemicals from which the model blanks were cast.

### CONCLUSIONS AND FUTURE PROGRAM

It is evident that these initial attempts to generate a photomechanical law emphasize numerous problems. The deviations in mechanical and optical properties of photoelastic materials in the glassy state seem to be magnified in the transition range between the glassy and the rubbery states. The exploratory attempts to derive a law on the basis of the data on the current program have been inconclusive.

The paths to be followed in undertaking further efforts appear to be revealed by the present results. It is apparently necessary to obtain accurate regulation of temperature and humidity during each test. Furthermore, repetitions of a specific test should be made on a single model, and conclusions should be withheld until reproducibility is obtained.

It is conceivable that the photoelastic plastic which was designed and fabricated especially for this program may be unsatisfactory and other materials might warrant investigation. Certainly if reproducibility is unobtainable with the current plastic, then such a search should be instituted.

The effect of the load history during dead weight loading should be evaluated. The influence of the manner of loading upon the observed mechanical properties of a photoviscoelastic plastic probably would require development of sophisticated instrumentation. It may also be necessary to eliminate all other possible causes of scatter in the data before this effect can be evaluated accurately.

Repeated annealing should be evaluated to determine whether this would have a significant influence upon both mechanical and optical properties in the transition range. Furthermore, various types of annealing cycles (including both short and extremely long times at annealing temperature) should be investigated.

The photoviscoelastic range appears to be closely related to the thermal expansion characteristics of a photoelastic plastic. A procedure has been developed<sup>11</sup> which permits highly accurate measurements of thermal expansion. Mechanical and optical property data should be correlated with these results.

### References

1. Mueller, H., *Physics*, **6**, No. 6, June 1935.
2. Mindlin, R. D., *Appl. Phys.*, **29**, 206 (1949).
3. Stein, R. S., S. Onogi, and D. A. Keedy, *J. Polymer Sci.*, **57**, 801 (1962).
4. Kawata, K., *J. Polymer Sci.*, **32**, 27 (1958).



5. Andrews, R. D., and J. F. Rudd, *J. Appl. Phys.*, **27**, 990 (1956); *ibid.*, **28**, 1091 (1957).
6. Theocaris, P. S., and C. Mylonas, *J. Appl. Mech.*, **28** (1961).
7. Goodman, L. E., and J. G. Sutherland, NACA TN 3043, November 1953.
8. Ferry, J. D., *Viscoelastic Properties of Polymers*, Wiley, New York, 1961.
9. Bland, D. R., *The Theory of Linear Viscoelasticity*, Pergamon Press, New York, 1960.
10. Weller, R., D. J. Middlehurst, and R. Steiner, NACA TN 841, February 1942.
11. Colao, A. C., and H. Becker, New York University Technical Report SM 62-9, August 1962.

### Résumé

On a procédé à des essais exploratoires sur un plastique photoviscoélastique spécialement conçu et fabriqué en vue de développer une expression de la relation entre l'ordre de frange et le comportement mécanique du plastique. A cause de la dépendance possible entre l'ordre de frange et les traction et tension internes, on a appelé cette relation "la loi photomécanique." Les résultats obtenus jusqu'à présent ne permettent pas de conclure. Par contre, on a mis en évidence de nombreux problèmes qui indiquent le type de programme qui pourrait conduire à une loi photomécanique.

### Zusammenfassung

Versuchstestes wurden an einem speziell entwickelten und erzeugten photoviscoelastischem Kunststoff durchgeführt, um die Form der Beziehung zwischen Fransenordnung und dem mechanischen Verhalten des Kunststoffes kennenzulernen. Wegen der möglichen Abhängigkeit der Fransenordnung von Spannung und Verformung wurde die Beziehung als "photomechanisches Gesetz" bezeichnet. Die bis jetzt erhaltenen Ergebnisse erlauben noch keine endgültigen Schlüsse. Es wurde zusätzlich eine grosse Zahl von Problemkreisen entdeckt, die erkennen lassen welches Versuchsprogramm zur Auffindung des photomechanischen Gesetzes führen kann.

Received October 8, 1962